Directional movement of rat prostate cancer cells in direct-current electric field: involvement of voltage-gated Na^+ channel activity

Mustafa B. A. Djamgoz[1,*], Maria Mycielska[1,2], Zbigniew Madeja[2], Scott P. Fraser[1] and Wlodzimierz Korohoda[2]

[1]Department of Biology, Imperial College of Science, Technology and Medicine, Sir Alexander Fleming Building, London, SW7 2AZ, UK
[2]Department of Cell Biology, Institute of Molecular Biology, Jagiellonian University, 31-120 Krakow, Poland
*Author for correspondence (e-mail: m.djamgoz@ic.ac.uk)

Accepted 12 April 2001
Journal of Cell Science 114, 2697-2705 (2001) © The Company of Biologists Ltd

SUMMARY

A two-part hypothesis has been tested, which proposes that (1) prostate cancer cells are galvanotactic (i.e. respond to an electric field by moving directionally) and (2) voltage-gated Na^+ channel activity, which was shown previously to be expressed specifically by strongly metastatic cells, controls galvanotaxis. Two well-defined rat ('Dunning') cell lines, originally derived from the same prostate tumour but differing markedly in their metastatic ability, were used. Cells were exposed to exogenous direct-current electric fields of physiological strength (0.1-4.0 V cm^{-1}), their reactions were recorded by light microscopy and analysed by a quantitative tracking method. Voltage-gated Na^+ channel activity was modulated pharmacologically using a range of concentrations of a specific channel blocker (tetrodotoxin) or an opener (veratridine). The results showed that the highly metastatic MAT-LyLu cells responded to the application of the electric field strongly by migrating towards the cathode. By contrast, the weakly metastatic AT-2 cells gave no such response. Tetrodotoxin suppressed the galvanotactic response of the MAT-LyLu cells whereas veratridine enhanced it. Both compounds had little effect on the AT-2 cells. These results are consistent with functional voltage-gated Na^+ channel expression occurring specifically in highly metastatic cells. This is also the first demonstration of control of galvanotaxis, in any cell type, by voltage-gated Na^+ channel activity. The possible underlying mechanisms and the in vivo relevance of these findings are discussed.

Key words: Cancer, Metastasis, Voltage-gated Na^+ channel, Prostate, Dunning, Rat

INTRODUCTION

Motility of cancer cells is important for the progression of metastasis because the cells have to migrate from primary sites, intra- or extravasate, and ultimately invade the target tissue to establish secondary tumours (reviewed by Mohler, 1993; Banyard and Zetter, 1999). A number of studies have demonstrated a strong correlation between cell motility (determined by membrane ruffling, pseudopod extensions and cell translocation) and metastatic potential (Mohler et al., 1987; Mohler et al., 1988; Partin et al., 1989). Cancer cells can respond in a motile fashion to many external factors including extracellular matrix components, host-derived motility and growth factors as well as tumour-derived autocrine agents (Levine et al., 1995) and scatter factors stimulating random (chemokinetic) or directional (chemotactic) motility of cancer cells (Aznavoorian et al., 1993).

A variety of motile cells, from protozoan to mammalian, also respond to an externally applied direct-current (DC) electric field by changing the orientation of their movement (Erickson and Nucitelli, 1984; Robinson, 1985; Ferrier et al., 1986; Frank and Gruler, 1990; Nishimura et al., 1996; McCaig and Zhao, 1997). This property, known as 'galvanotaxis', is involved in a number of basic biological processes, such as embryonic development (Jaffe and Nucitelli, 1977; McCaig, 1989a; McCaig, 1989b; McCaig and Dover, 1989) and can also manifest itself under pathophysiological conditions, as in wound healing (e.g. Chiang et al., 1992). In the related phenomenon of 'galvanotropism', external electric fields can facilitate cellular process extension, again in both normal conditions (e.g. Hotary and Robinson, 1990) and pathological situations (e.g. bone healing; Zhuang et al., 1997) and nerve regeneration (Borgens et al., 1981). However, it is not known whether cancer cells are galvanotactic. Also, it is not known whether there is any relation between galvanotaxis and metastatic potential. Nevertheless, metastasis can involve specific tissue invasion; for example, rat prostate cancer MAT-LyLu cells metastasise specifically to lymph nodes and lungs (Isaacs et al., 1986). Furthermore, metastasis can originate from sites in the body (e.g. epithelial ducts, skin) where local DC electric fields would occur. In the case of the rat prostate gland, a transepithelial potential of some −10 mV has been recorded (Szatkowski et al., 2000). Interestingly, electro-imaging of mammary and cervical tissues has been used in clinical detection of malignancy (Fukuda et al., 1996; Faupel et al., 1997; Cuzick et al., 1998), although its basis is not well understood.

Cells can react to an applied weak DC electric field in different ways, moving towards the cathode or the anode, and it is possible that a variety of membrane mechanisms are

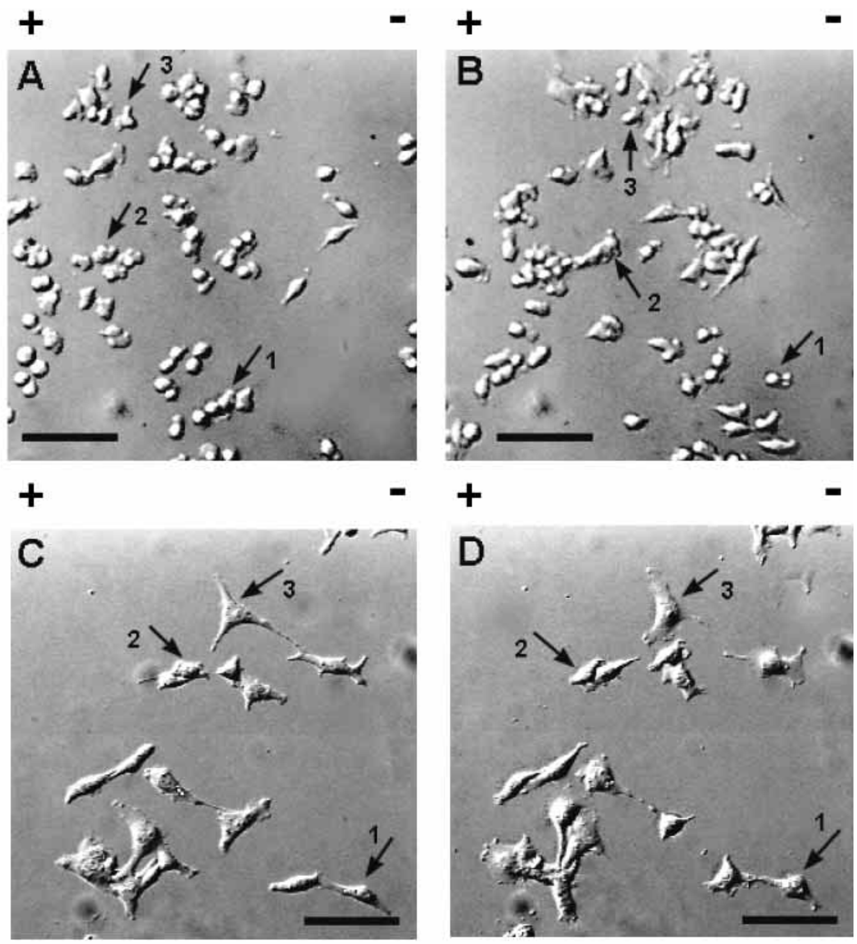

Fig. 1. Typical time-lapse photographs showing translocation of MAT-LyLu (A,B) and AT-2 (C,D) cells in electric fields (3 V cm^{-1}); polarity indicated with '+' (anode) and '–' (cathode). (A) Image of MAT-LyLu cells immediately after turning the electric field on (time=0), with the positions of three typical cells indicated (1-3). (B) The same field of view as in (A) taken 2 hours later. It is clear that the cells have moved significantly towards the cathode. (C) Images of AT-2 cells at time=0, with the positions of three cells indicated (1-3). The same field of view as in (C) taken 2 hours later, indicating insignificant movement of cells. Bars, 100 μm.

involved in such responses (e.g. Nuccitelli, 1988; Robinson, 1985; Soong et al., 1990). It has been observed that, under the influence of externally applied DC electric fields, Ca^{2+} concentration increased significantly and was maintained for the duration of exposure (Onuma and Hui, 1988). In this situation, the cell would move away from the end where intracellular Ca^{2+} rises and contractile activity occurs (Cooper and Keller, 1984). Accordingly, in the presence of Ca^{2+} channel blockers (e.g. D-600, verapamil), the directionality of migration can be disturbed and replacement of external Ca^{2+} by Mg^{2+} can also reverse the electrotactic response (Cooper and Schliwa, 1986; Onuma and Hui, 1988; Nuccitelli and Smart, 1989). Importantly, however, Ca^{2+}-independent control of galvanotaxis has also been found (e.g. Brown and Loew, 1994; Palmer et al., 2000), and it is not clear whether other ionic mechanisms also play a role in galvanotactic responses of cells. We have shown previously that there are distinct electrophysiological differences between strongly and weakly metastatic cells of rat and human prostate carcinoma (Grimes et al., 1995; Laniado et al., 1997; Smith et al., 1998; Foster et al., 1999). In particular, functional voltage-gated Na^+ channels (VGSCs) occurred specifically in the highly metastatic cells (Grimes et al., 1995; Laniado et al., 1997; Grimes and Djamgoz, 1998). Indeed, VGSC expression and invasiveness in vitro were correlated in numerous rat and human prostate cancer cell lines (Smith et al., 1998).

Taking the available evidence together, the possibility arises that metastatic cells could be galvanotactic and that membrane ion channel (VGSC) activity could play a role in this process. The present study aimed to evaluate this overall hypothesis. In order to test the possible involvement of VGSC activity in galvanotactic reaction, tetrodotoxin (TTX), a highly specific blocker of VGSCs, was used. The working concentration of TTX was 1 μM, which would effectively block the TTX-sensitive VGSCs present in the strongly metastatic MAT-LyLu line (Grimes and Djamgoz, 1998; Diss et al., 2001). A further, 'opposite' test was carried out using veratridine (a VGSC 'opener'), which potentiates VGSC activity by lowering the threshold of the activation voltage (Eskinder et al., 1993). Finally, possible involvement of voltage-gated Ca^{2+} channels was tested using verapamil as a general blocker (Cooper and Schliwa, 1986).

MATERIALS AND METHODS

Cell culture

Experiments were carried out on two well characterised rat prostate cancer ('Dunning') cell lines having markedly different metastatic ability: MAT-LyLu and AT-2 cells which metastasise in >90% and <10% of cases, respectively, when injected into Copenhagen rats (Isaacs et al., 1986). The cells were cultured at a density of ~100,000 cells cm^{-2}, as described previously (Grimes et al., 1995), except that the concentration of fetal calf serum (FCS; Sigma) was increased to 5% to facilitate cell attachment. Cultures were always used 24 hours after plating, when single cells were abundant.

Galvanotaxis

Migration was assayed using a galvanotaxis apparatus described in detail by Korohoda et al. (Korohoda et al., 2000). Essentially, this was made up from a glass observation chamber comprising a sandwich of two glass coverslips (with the cells free to move in between) mounted in a Plexiglas holder. Direct current was applied for 6 hours, through Ag/AgCl reversible electrodes (of 6 cm^2 surface area) immersed in wells filled with cultured medium (RPMI + 5% FCS). Each well was connected by an agar bridge to a neighbouring pool, which was continuous with the observation chamber. The cover-glasses composing the latter measured 60 mm×5 mm×0.2 mm. The electric current flowing through the chamber was measured continuously with a milliampermeter; the voltage gradient was calculated using Ohm's Law and confirmed by measuring with a high-input impedance

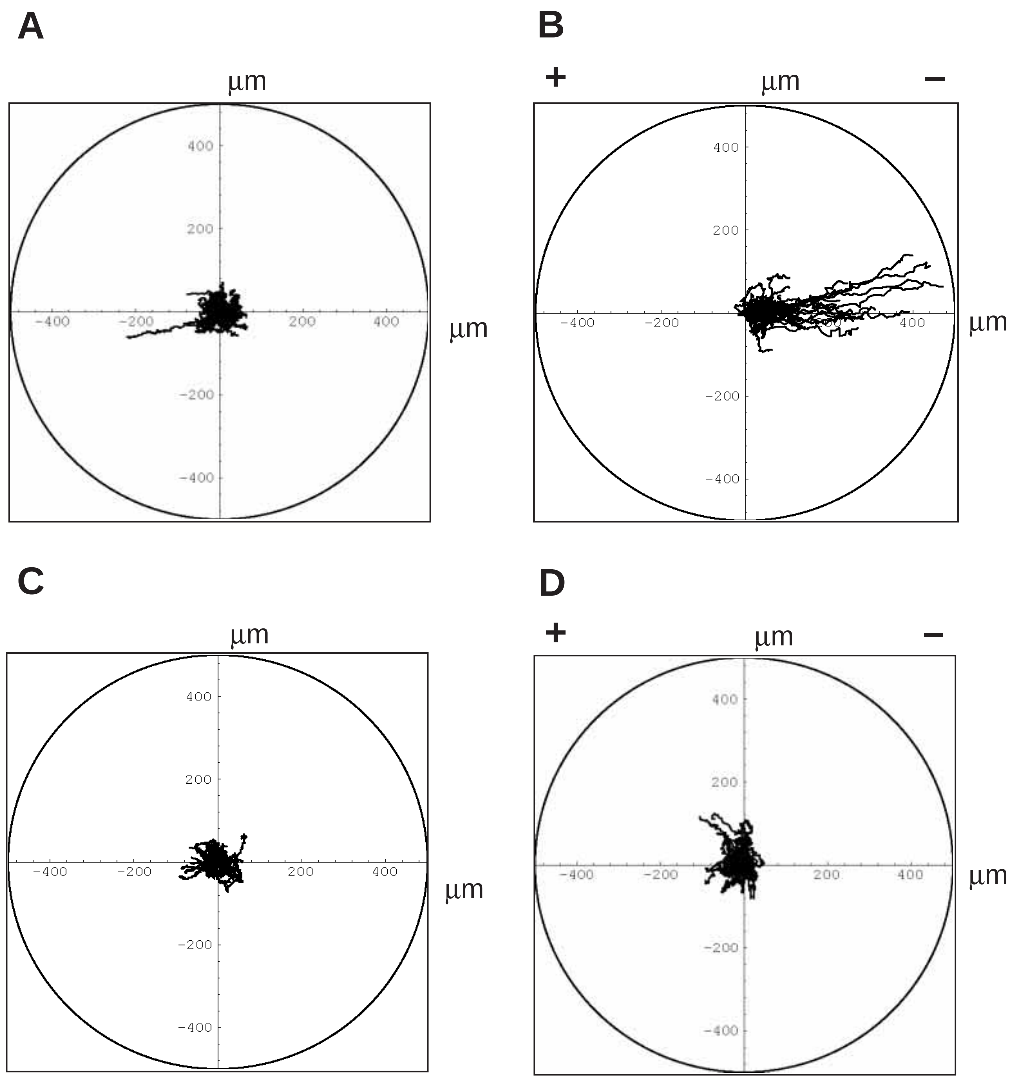

Fig. 2. Composite trajectories of 50 MAT-LyLu (A,B) and AT-2 cells (C,D) migrating in the absence (A,C) and in the presence (B,D) of an electric field (3 V cm^{-1}), shown as circular diagrams. In each diagram, the initial point for each trajectory was placed at the centre of the circle. The *x* axis corresponds to the direction of the electric field. The cathode ('−' pole) was always placed at the right-hand side of the diagram.

voltmeter (Korohoda and Kurowska, 1970; Cho et al., 1996). 24 hours before starting an experiment, the cells were re-plated onto one of the glass covers. At the beginning of the experiment, this was sandwiched onto a second plate (with a 0.2 mm gap, the cells still being bathed in their normal growth medium), sealed with silicone grease and mounted in the Plexiglas apparatus. Observations were carried out on an inverted microscope (Olympus, IMT-2). Cells were observed using phase contrast optics at a total magnification of 285× (corresponding to a field of view of 710×710 μm). All experiments were done at 37°C (the temperature of the chamber was monitored and found to remain constant). Analysis of cells' motility during the experiment (6 hours) confirmed that the recording conditions were very stable because there was no observable change in any parameter under the control conditions. All experiments were carried out for 6 hours unless otherwise stated.

Cell images were recorded with a Hitachi CCD camera, digitized and processed with the computer programs as described previously (Korohoda and Madeja, 1997; Korohoda et al., 1997a; Korohoda et al., 1997b). For cell motion tracking, a series of time-lapse images of cells were acquired using a frame-grabber device and a 'slow motion VCR' program (VCR 1.0). The cell trajectories were constructed from 72 successive cell centroid positions recorded over 6 hours with a time interval of 5 minutes (30 seconds in some experiments). For each experimental condition, the trajectories of at least 50 cells were analysed. Usually, 15-20 cells were examined in one experiment and data from three or four experiments were pooled. Detailed analyses of the data were performed using the program 'Mathematica' (Wolfram Research Inc., Champaign, IL; Korohoda and Madeja, 1997; Korohoda et al., 1997a).

Parameters

The following parameters characterising different aspects of cell locomotion were computed and analysed for each cell or cell population (Korohoda et al., 2000).

(1) Total length of cell trajectory (TLT). This was essentially the 'true' length of the path (in μm) travelled by the cell. The value of TLT was calculated from the sequence of *n* straight-line segments, each corresponding to a cell-centroid translocation between two successive images.

(2) Average speed of cell locomotion (ASL). This was defined as the total length of cell trajectory (TLT) ÷ time of recording (6 hours).

(3) Total length of cell displacement (TLD). This was the distance (in μm) from the starting point direct to the final position of the cell.

(4) Average rate of cell displacement (ARD). This was defined as the total length of cell displacement from the starting point to the final cell position (TLD) ÷ time of recording (6 hours).

(5) Coefficient of movement efficiency (CME). This was defined as the ratio of total cell displacement (TLD) to total cell trajectory length (TLT). The value of CME would be 1 for cells moving persistently along one straight line in one direction, and 0 for random movement (Friedl et al., 1993; Korohoda et al., 1997b).

(6) Average directional cosine γ (ADCγ). The angle γ was defined as the directional angle between the *x* axis (parallel to the electric field) and a vector AB, A and B being the original and each subsequent positions of the cell, respectively. This parameter would equal +1 for a cell moving towards the cathode, −1 for a cell moving in the direction of the anode and 0 for random movement (Gruler and Nuccitelli, 1991; Korohoda et al., 1997b). This parameter was used generally to quantify the directionality of movement.

(7) Average directional cosine β (ADCβ). The angle β was defined as the directional angle between the *x* axis (parallel to the electric field) and a vector AB, A and B being two successive positions of the

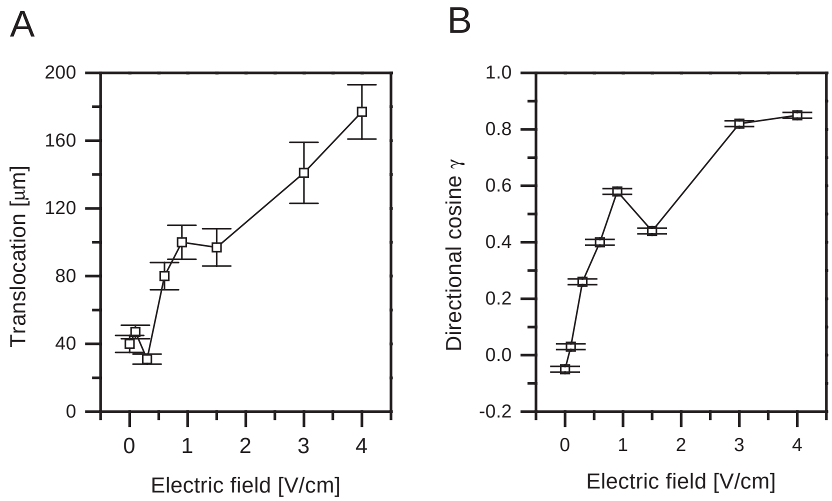

Fig. 3. Effects of increasing the strength of electric field (in the range 0.1-4.0 V cm^{-1}) on two parameters of galvanotaxis (as defined in the text) measured in MAT-LyLu cells. (A) Translocation (total length of cell displacement in µm). (B) Directional cosine γ (average directional cosine γ; ADCγ). Data points denote means ± s.e.m. (*n*=50). The measurements were made after 6 hours exposure to the electric field.

cell, respectively. This parameter would equal +1 for a cell moving towards the cathode, −1 for a cell moving in the direction of the anode and 0 for random movement (Gruler and Nuccitelli, 1991; Korohoda et al., 1997b). This parameter was particularly useful in testing the reversibility of effects of electric field or a given pharmacological agent.

Pharmacology

In experiments involving pharmacological treatment of the cells under investigation, a given test compound was introduced into the observation chamber and recording started immediately. In some experiments, it was possible to re-perfuse the cells with the control medium while recording to check the reversibility of the effect, if any. The following compounds were used: TTX (citrate free), veratridine and verapamil. All chemicals were obtained from Sigma-Aldrich.

Data analysis

Data are presented as means ± s.e.m. Statistic significance was determined using the Mann-Whitney test. Values of $P < 0.01$ were assumed to represent significance.

RESULTS

Under the culture conditions used, there were some noticeable differences between the morphologies of the strongly metastatic MAT-LyLu and the weakly metastatic AT-2 cells (Fig. 1). The MAT-LyLu cells were more rounded and the population was more heterogeneous (Fig. 1A,B). By contrast, the AT-2 cells were much flatter, with processes that spread out and attached to the surface (Fig. 1C,D). The quantitative motility data obtained for MAT-LyLu and AT-2 cells are summarised in Tables 1 and 2, respectively. In the absence of any external electric field, the MAT-LyLu and AT-2 cells migrated laterally in culture with comparable speeds (52-57 µm hour^{-1}) and random directionality (ADCγ=–0.04 to –0.05) (Fig. 2A,C). A dramatic change occurred in the MAT-LyLu cells following application of an electric field of 3 V cm^{-1}, whereby their movement became strongly directional (ADCγ=0.82), cells turning to move almost linearly towards the cathode (Fig. 2A,B). Thus, although the average speed of movement was not affected, the rate of cell displacement increased nearly fourfold (Table 1). This effect was very rapid, microscopically detectable changes occurring within 30 seconds (i.e. between successive frames in the fast time-lapse recordings) after applying the field. By contrast, the AT-2 cells showed no such response (Fig. 2C,D; Table 2). In fact, there was a tendency for the AT-2 cells to move in the opposite direction but this was not studied further.

The electric field effects seen on the motility of the MAT-LyLu cells were enhanced as the applied voltage gradient was made stronger (Fig. 3A,B). Thus, as the electric field was increased from 0.1 V cm^{-1} to 4.0 V cm^{-1}, both the directionality of movement and the overall length of cell displacement increased steadily. These effects were reversible. Thus, upon extinguishing or reversing the field, the cells' corresponding responses were rapidly abolished or reversed, respectively (Fig. 4). On the whole, however, there was some

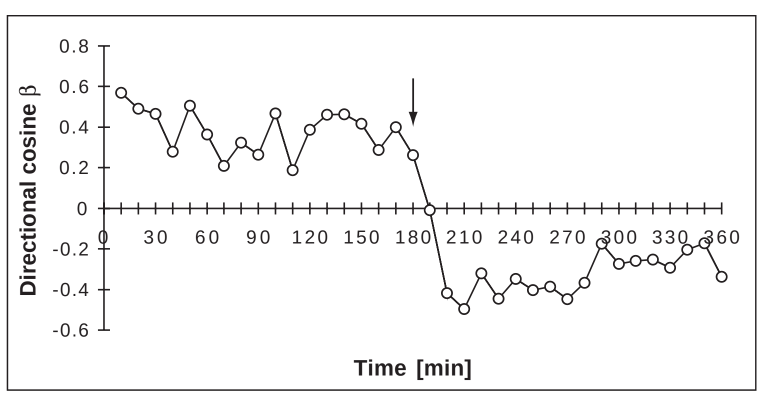

Fig. 4. A typical result showing the reversibility of the effect of an applied electric field (3 V cm^{-1}) on the galvanotactic response of MAT-LyLu cells. The graph shows the plot of the average cosine of directional segmental angle β calculated from 50 trajectories against time. The segment corresponds to the distance covered by the cell in 10 minute intervals. The field was reversed after 3 hours of recording, at the point marked by the arrow. Positive values of β corespond to cathodal movement of cells.

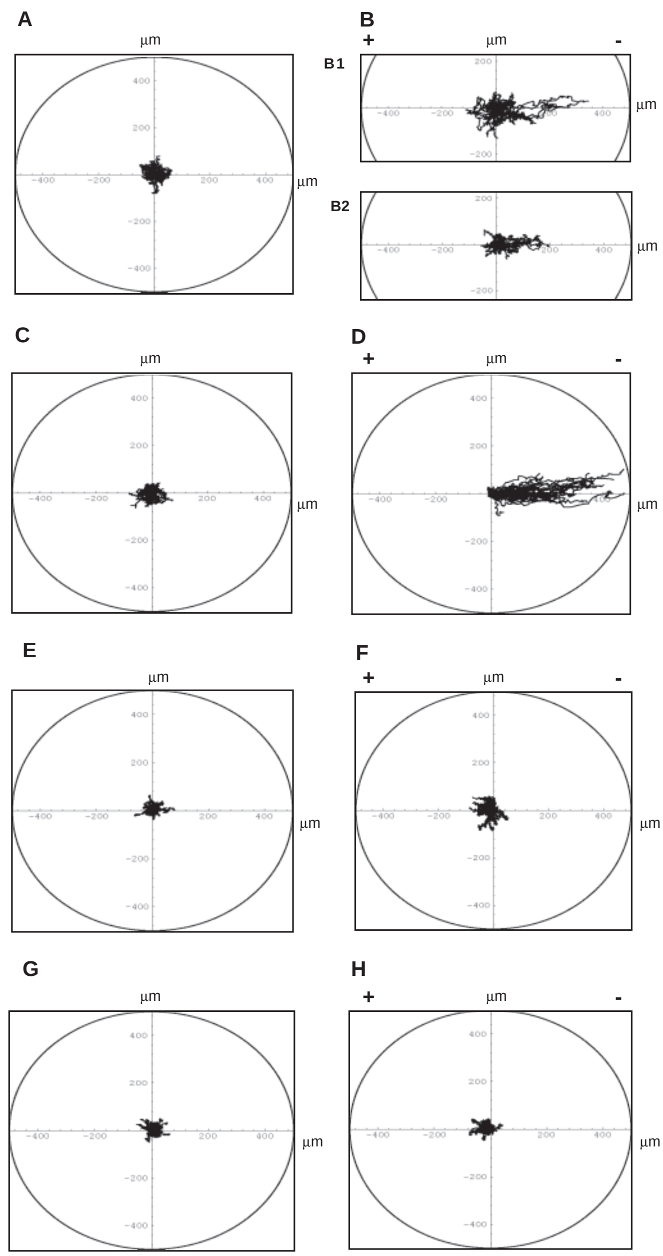

Fig. 5. Effects of pharmacological blockage and potentiation of VGSC activity on galvanotactic responses of MAT-LyLu (A-D) and AT-2 cells (E-H). Data are plotted as in Fig. 3. The experimental conditions in the treatments were as follows. (A) MAT-LyLu cells, 1 μM TTX, no electric field. (B) MAT-LyLu, 1 μM TTX (B1) or 5 μM TTX (B2), electric field of 3 V cm^{-1}. (C) MAT-LyLu cells, 10 μM veratridine, no electric field. (D) MAT-LyLu cells, 10 μM veratridine, electric field of 3 V cm^{-1}. (E) AT-2, 1 μM TTX, no electric field. (F) AT-2, 1 μM TTX, electric field of 3 V cm^{-1}. (G) AT-2, 10 μM veratridine, no electric field. (H) AT-2, 10 μM veratridine, electric field of 3 V cm^{-1}.

heterogeneity in the cells' response to the electric fields, with small, rounded cells appearing more sensitive than larger cells with prominent extensions.

We have shown previously that only strongly metastatic cells express functional VGSCs (Grimes et al., 1995; Laniado et al., 1997; Smith et al., 1998). Therefore, the possible role of VGSC activity in the cells' response to electric field was investigated by pharmacological manipulation of VGSC activity (Grimes and Djamgoz, 1998; Fraser et al., 2000; Figs 5-7; Tables 1, 2). An additional parameter, P_c (percentage of cells crossing a criterion boundary of 200 μm from the position occupied just before application of the field during the 6-hour recording period) was used to compare the effects of the drugs on the extent of the cells' directional migration (Fig. 7). Under control conditions, only very few (~2%) MAT-LyLu cells crossed the barrier; this was greatly facilitated by the electric field (P_c=24.0±2.9%; P=0.001) (Fig. 7), consistent with the demonstration above. None of the AT-2 cells migrated to this extent (Fig. 2C; Fig. 5E). Treatment of the MAT-LyLu cell cultures with verapamil (1-10 μM) produced no effect (not illustrated). However, the specific VGSC blocker TTX at 1 μM noticeably reduced the percentage of MAT-LyLu cells migrating over the 200 μm criterion distance (P_c=7.6±4.3%), whereas 2.5-5 μM TTX blocked the effect of the field completely (P_c=0%) (Fig. 5A,B; Fig. 7). The effects of TTX were reversed by washing the cells with the control medium (Fig. 6). TTX had very little effect on the average speed of movement of the MAT-LyLu cells (Table 1) or any of the measured parameters of the AT-2 cells (Table 2; Fig. 5E,F).

Potentiating VGSC activity with veratridine (VER) had the opposite effect to TTX, enhancing the specific actions of the electric field treatment on the MAT-LyLu cells (Fig. 5C,D; Fig. 7). Thus, in the presence of 1 μM VER, the coefficient of movement efficiency increased significantly from the normal value of 0.34 to 0.62 without any effect on the average speed of cell movement (Table 1), and 30.0 ± 10% of cells crossed the 200 μm criterion barrier (Fig. 7). The effects of VER were dose-dependent (Table 1; Fig. 7). The value of ADCγ was enhanced significantly at 5 μM, the cells increasing their directional response further than with application of the field alone. At the highest concentration of VER used (10 μM), P_c=44.0±2.0% (P=0.002 compared with electric field without VER) (Fig. 7). Cell viability, assessed by trypan blue staining, was not affected by VER (10 μM) or TTX (5 μM). However, VER treatment again had relatively little effect on the AT-2 cells (Table 2), consistent with functional VGSCs being absent in these cells.

DISCUSSION

The results of the present study show for the first time that prostate cancer cells can be galvanotactic and that VGSCs are involved in galvanotactic response, both aspects being correlated with metastatic potential (Grimes et al., 1995; Laniado et al., 1997; Smith et al., 1998). Thus, the hypothesis under investigation has been confirmed.

The galvanotactic responses of various cell types, including neurons and epithelia, have been found to be cathodal (McCaig and Zhao, 1997; Palmer et al., 2000), as shown here for the MAT-LyLu cells. The effect is unlikely to be due to any asymmetry in the distribution of VGSC protein over the cell surface because this was found to be uniform on MAT-LyLu cells (not shown). Furthermore, any gross redistribution of VGSCs (or other protein) in the membrane by electrophoresis would also seem to be unlikely because this would take hours (Jaffe, 1977), or at least several minutes (Fang et al., 2000),

Table 1. Quantitative data showing the effects of electric field and various pharmacological treatments on MAT-LyLu cells*

Parameters	Control	1 µM TTX	10 µM Veratridine	Electric field (3 V cm^{-1})	Electric field (3 V cm^{-1}) + 1 µM TTX	Electric field (3 V cm^{-1}) + 5 µM TTX	Electric field (3 V cm^{-1}) + 1 µM veratridine	Electric field (3 V cm^{-1}) + 5 µM veratridine	Electric field (3 V cm^{-1}) + 10 µM veratridine
Total length of cell trajectory (TLT) (µm)	343±7	329±8.4	344±8.3	369±13	375±11	322±9.6	258±13	377±16	470±18
Average speed of cell movement (ASL) (µm h^{-1})	57±1.2	54±1.4	57±1.4	60±2.1	62±1.8	53±1.6	43±6.1	63±2.6	78±3
Total length of cell displacement (TLD) (µm)	40±4.7	26±2.4	26±2.9	141±18	86±8.7	50±6.6	165±11.2	189±16	202±19
Average rate of cell displacement (ARD) (µm h^{-1})	6.7±0.8	4.3±0.4	4.3±0.5	23.6±3	14±1.4	8.3±1.1	27±1.9	31±2.6	34±3.2
Coefficient of movement efficiency (CME)	0.11±0.01	0.08±0.01	0.07±0.01	0.34±0.003	0.21±0.02	0.15±0.02	0.62±0.03	0.46±0.02	0.39±0.03
Average directional cosine γ (ADCγ)	–0.05±0.01	0.12±0.01	–0.12±0.01	0.82±0.01	0.26±0.01	0.42±0.01	0.78±0.01	0.86±0.01	0.88±0.01

*Data are presented as mean±s.e.m. Definitions of the parameters and details of the statistics are given in the text.

Table 2. Quantitative data showing the effects of electric field and various pharmacological treatments on AT-2 cells*

Parameters	Control	1 µM TTX	10 µM Veratridine	Electric field (3 V cm^{-1})	Electric field (3 V cm^{-1}) + 1 µM TTX	Electric field (3 V cm^{-1}) + 5 µM TTX	Electric field (3 V cm^{-1}) + 5 µM veratridine	Electric field (3 V cm^{-1}) + 10 µM veratridine
Total length of cell trajectory (TLT) (µm)	312±7.4	296±6.8	292±7.2	344±8.2	349±7.1	255±6.1	294±7.5	271±8
Average speed of cell movement (ASL) (µm h^{-1})	52±1.2	49±1.1	49±1.2	57±1.4	58±1.2	42±1	49±1.2	45±1.3
Total length of cell displacement (TLD) (µm)	37±3.3	20±1.8	24±2.2	45±4.6	39±3.4	45±3.2	40±3.5	41±2.7
Average rate of cell displacement (ARD) (µm h^{-1})	6.2±0.5	3.3±0.3	3.9±0.4	7.5±0.8	6.5±0.6	7.5±0.5	6.6±0.6	6.7±0.4
Coefficient of movement efficiency (CME)	0.12±0.01	0.07±0.01	0.08±0.01	0.13±0.01	0.11±0.01	0.18±0.01	0.13±0.01	0.16±0.01
Average directional cosine γ (ADCγ)	–0.04±0.01	0.07±0.01	0.27±0.01	–0.34±0.01	–0.38±0.01	–0.5±0.01	–0.4±0.01	–0.6±0.01

*Data are presented as mean±s.e.m. Definitions of the parameters and details of the statistics are given in the text.

whereas the electric field produced an observable morphological change and directional response in the cells within 30 seconds. The following possibilities can be considered as underlying mechanisms.

Basic transmembrane Ca^{2+} influx

It has been observed that, under the influence of externally applied DC electric fields, intracellular Ca^{2+} concentration increased significantly and was maintained for the duration of exposure (Onuma and Hui, 1988; Perret et al., 1999). In the simplest case, of a cell devoid of voltage-gated (depolarization-activated) Ca^{2+} channels (VGCCs), passive influx of Ca^{2+} and contraction would on the anodal side and the cell would move towards the cathode. In cells with VGCCs, however, Ca^{2+} influx would (also) occur on the cathodal, depolarised, side; thus, the direction of movement might depend on the balance between the two sites of intracellular Ca^{2+} rise. These possibilities are unlikely to be directly applicable here for several reasons. (1) Any simple passive Ca^{2+} influx should have affected the two cell types similarly but this was not seen (Fig. 2B,D). (2) Verapamil (a general blocker of Ca^{2+} channels) was found not to affect the galvanotactic response of the cells. (3) The membrane depolarisation caused directly by the electric field should have facilitated Ca^{2+} channel activation directly without involving VGSCs; that is, TTX should not have had any effect. (4) Our preliminary patch-clamp recordings and intracellular Ca^{2+} measurements suggest, in fact, that the MAT-LyLu cells do not possess voltage-gated Ca^{2+} channels (or significant Na^{+}-Ca^{2+} exchanger activity).

Surface charge

The ‘direct’ effect of the electric field on the membrane potential could be compounded by the presence of a negative surface charge, which is known to occur in cancer cells and to increase in line with metastatic potential (Abercrombie and Ambrose, 1962; Carter and Coffey, 1988; Carter et al., 1989; Price et al., 1987). It is therefore possible that, in the presence of the exogenous electric field, the charge ‘cloud’ would be asymmetrical, and this could generate a spatial variation in membrane potential (Gross, 1988; Heberle et al., 1994; Scherrer, 1995) that is different between the two cell types. In the case of the MAT-LyLu cells, the negative charges could accumulate on the anodal surface, thereby depolarising the cell membrane. This could then simply increase the passive influx of Ca^{2+}, leading to contraction on the anodal side and propulsion of the cells towards the cathode, as has been observed (Bedlack et al., 1992; Olivotto et al., 1996). In addition, the VGSCs could interact directly with the cytoskeleton (Sheng and Kim, 1996), possibly by the membrane depolarisation inducing repeated conformational changes in the VGSC proteins. Furthermore, VGSC β-subunits possess a cell-adhesion motif (e.g. Isom et al., 1995) and this could facilitate interaction with the extracellular matrix. We should also note that control of galvanotaxis by Ca^{2+} released from internal stores (Rosado and Sage, 2000) and other more elaborate secondary messenger have also been proposed (McCaig and Zhao, 1997). However, how these could

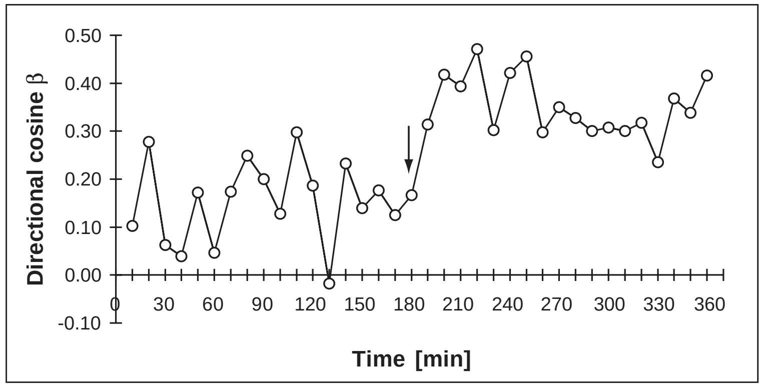

Fig. 6. Reversibility of the effect of TTX on the galvanotactic behaviour of MAT-LyLu cells in an electric field of 3 V cm^{-1}. The experiments started with the cells just treated with the toxin (5 μM) whereby the average cosine of directional segmental angle β (calculated from 50 trajectories) was near zero (i.e. there was little directionality in the movement). The toxin was washed after 3 hours of recording (at the moment indicated by the arrow), whereupon the directionality of response was restored. Other details as in Fig. 5.

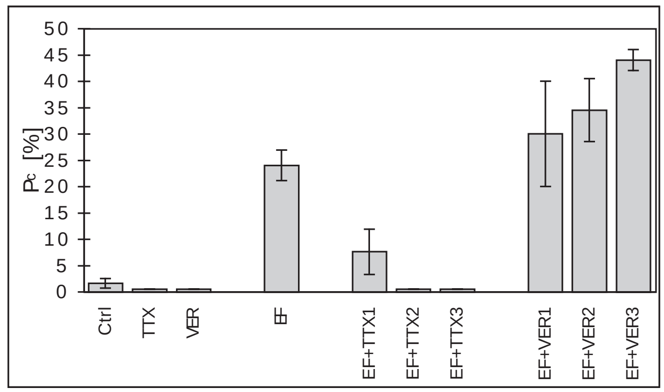

Fig. 7. Percentage of MAT-LyLu cells crossing a criterion boundary 200 μm (P_c) from the original position occupied just before turning the electric field (EF) on. The first three bars from the left-hand side represent the various control conditions without electric field: Ctrl, control (with no field or pharmacology); TTX, 1 μM tetrodotoxin (TTX); VER, 10 μM veratridine (VER). The fourth bar shows data for application of electric field alone. The bars next on the right represent values of P_c for cells moving in the electric field in the presence of various concentrations of TTX or VER. Concentrations: TTX1, 1 μM; TTX2, 2.5 μM; TTX3, 5 μM; VER1, 1 μM; VER2, 5 μM; VER3, 10 μM. Each mean value was calculated from three or four separate experiments. Error bars represent s.e.m.

involve VGSC activity is not clear at present. We also do not know whether electric field treatment could have any long-term effect. Further work is required to evaluate these possibilities.

The hitherto unknown role of VGSC activity in galvanotaxis that we have demonstrated could have important implications in both cellular physiology and pathophysiology. First, as regards normal biological functioning, a variety of basic processes do involve directional or patterned growth, including target-specific axonal migration and patterning of regional synaptic connectivity. These processes have frequently been shown to be blocked by TTX treatment, so would appear to depend on VGSC activity (Dubin et al., 1986; Catalano and Shatz, 1998; Meyer, 1982; Penn et al., 1998; Shatz, 1990). Accordingly, VGSC expression and activity in cells exposed to endogenous electric fields could facilitate directional growth in vivo.

Second, assuming that our findings are also applicable to the situation in vivo (Fig. 8), especially because VGSC protein is produced in clinical tumours at levels correlated with pathological grading (Stewart et al., 1999), it would follow that the directional migration of prostate cells during the early stages of metastasis could be influenced significantly by endogenous transepithelial potentials (TEPs). We have recently found that rat prostate epithelia have a lumen potential of about −10 mV (Szatkowski et al., 2000). Such a lumen potential would correspond to transepithelial voltage gradient of 5 V cm^{-1}, assuming that the cellular thickness of the prostatic ducts is 20 μm (Fig. 8). Such a voltage gradient is comparable to the DC electric field strengths used to induce galvanotaxis in the present study. If a similar situation occurs in the human prostate epithelium in vivo then it would follow that presumed premetastatic cells with VGSC activity would tend to migrate into the lumen and be detectable in the semen (Gardiner et al., 1996; Barren et al., 1998). Subsequently, as metastatic

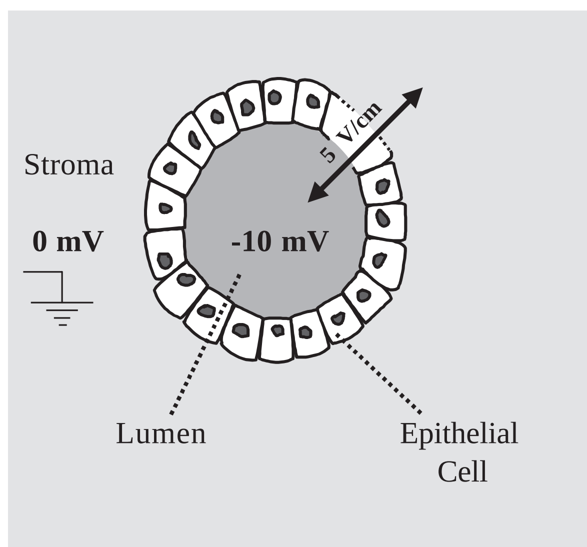

Fig. 8. A schematic diagram showing the basic cellular organisation of a prostatic epithelial duct with a prevailing lumen potential of −10 mV, relative to the stroma at earth potential (0 mV) (Szatkowski et al., 2000). Assuming the thickness of the epithelial cell layer to be 20 μm, the transcellular voltage gradient would be equivalent to 5 V cm^{-1}, as indicated. Thus, under these electrophysiological conditions, epithelial cells expressing functional VGSCs would be expected to migrate towards the lumen.

behaviour progressed, accompanied by deformation of the epithelia, the negative TEP would degrade, cellular migration into lumen would slow down and might even reverse, encouraging invasion of the surrounding tissue. Furthermore, the transendothelial potential (Revest et al., 1993) could similarly influence extra- and intravasation of circulating metastatic cells, which might be a critical step in metastasis (Wyckoff et al., 2000).

This study has been supported by the Prostate Cancer Research Fund (UK) and the Committee for Scientific Research (KBN, Poland). We thank Clare Isacke and Jimmy Diss for previewing the manuscript, and Andrew Goldsworthy and Marek Szatkowski for many useful discussions.

REFERENCES

Abercrombie, M. and Ambrose, E. J. (1962). The surface properties of cancer cells: a review. *Cancer Res*. **22**, 25-548.

Aznavoorian, S., Murphy, A. N., Stetler-Stevenson, W. G. and Liotta, L. A. (1993). Molecular aspects of tumor cell invasion and metastasis. *Cancer* **71**, 1368-1383.

Banyard, J. and Zetter, B. R. (1999). The role of cell motility in prostate cancer. *Cancer Metastasis Rev*. **17**, 449-458.

Barren, R. J., III, Holmes, E. H., Boynton, A. L., Gregorakis, A., Elgamal, A.-A. A., Cobb, O. E., Wilson, C. L., Ragde, H. and Murphy, G. P. (1998). Method for identifying prostate cells in semen using flow cytometry. *Prostate* **36**, 181-188.

Bedlack, R. S., Jr, Wei, M. and Loew, L. M. (1992). Localised membrane depolarisations and localised calcium influx during electric field-guided neurite growth. *Neuron* **9**, 393-403.

Borgens, R. B., Roeder, E. and Cohen, M. J. (1981). Enhanced spinal cord regeneration in lamprey by applied electric fields. *Science* **213**, 611-617.

Brown, M. J. and Loew, L. M. (1994). Electric field-directed fibroblast locomotion involves cell surface molecular organization and is calcium independent. *J. Cell Biol*. **127**, 117-128.

Carter, H. B. and Coffey, D. S. (1988). Cell surface charge in predicting metastatic potential of aspirated cells from the Dunning rat prostatic adenocarcinoma model. *J. Urol*. **140**, 173-175.

Carter, H. B., Partin, A. W. and Coffey, D. S. (1989). Prediction of metastatic potential in an animal model of prostate cancer: flow cytometric quantification of cell surface charge. *J. Urol.* **142**, 1338-1341.

Catalano, S. M. and Shatz, C. J. (1998). Activity-dependent cortical target selection by thalamic axons. *Science* **281**, 559-562.

Chiang, M., Robinson, K. R. and Vanable, J. W., Jr (1992). Electrical fields in the vicinity of epithelial wounds in the isolated bovine eye. *Exp. Eye Res.* **54**, 999-1003.

Cho, M. R., Thatte, H. S., Lee, R. C. and Golan, D. E. (1996). Reorganization of microfilament structure induced by ac electric fields. *FASEB J.* **10**, 1552-1558.

Cooper, M. S. and Keller, R. E. (1984). Perpendicular orientation and directional migration of amphibian neural cells in DC electrical fields. *Proc. Natl. Acad. Sci. USA* **81**, 160-164.

Cooper, M. S. and Schliwa, M. (1986). Motility of cultured fish epidermal cells in the presence and absence of direct current electric fields. *J. Cell Biol.* **102**, 1384-1399.

Cuzick, J., Holland, R., Barth, V., Davies, R., Faupel, M., Fentiman, I., Frischbier, H. J., LaMarque, J. L., Merson, M., Sacchini, V. et al. (1998). Electropotential measurements as a new diagnostic modality for breast cancer. *Lancet* **352**, 359-363.

Diss, J. K. J., Archer, S. N., Hirano, J., Fraser, S. P. and Djamgoz, M. B. A. (2001). Expression profiles of voltage-gated Na^+ channel α-subunit genes in rat and human prostate cancer cell lines. *Prostate* (in press).

Dubin, M. W., Stark, L. A. and Archer, S. M. (1986). A role of action-potential activity in the development of neuronal connections in the kitten retinogeniculate pathway. *J. Neurosci*. **6**, 1021-1036.

Erickson, C. A. and Nucitelli, R. (1984). Embryonic fibroblast motility and orientation can be influenced by physiological electric fields. *J. Cell Biol*. **98**, 296-307.

Eskinder, H., Supan, F. D., Turner, L. A., Kampine, J. P. and Bosnjak, Z. J. (1993). The effects of halothane and isoflurane on slowly inactivating sodium current in canine cardiac Purkinje cells. *Anesth. Analg.* **77**, 32-37.

Fang, K. S., Ionides, E., Oster, G., Nucitelli, R and Isseroff, R. R. (1999). Epidermal growth factor receptor relocalization and kinase activity are necessary for directional migration of keratinocytes in DC electric fields. *J. Cell Sci.* **112**, 1967-1978.

Faupel, M., Vanel, D., Barth, V., Davies R., Fentiman, I. S., Holland, R., Lamarque, J. L., Sacchini, V. and Schreer, I. (1997). Electropotential evaluation as a new technique for diagnosing breast lesions. *Eur. J. Radiol*. **24**, 33-38.

Ferrier, J., Ross, S. M., Kanehisa, J. and Aubin, J. E. (1986). Osteoclasts and osteoblasts migrate in opposite directions in response to a constant electrical field. *J. Cell Physiol.* **129**, 283-288.

Foster, C. S., Cornford, P., Forsyth, L., Djamgoz, M. B. A. and Ke, Y. (1999). The cellular and molecular basis of prostate cancer. *Br. J. Urol*. **83**, 171-194.

Frank, K. and Gruler, H. (1990). Galvanotaxis of human granulocytes: electric field jump studies. *Eur. Biophy. J*. **18**, 335-346.

Fraser, S. P., Grimes, J. A. and Djamgoz, M. B. A. (2000). Effects of voltage-gated ion channel modulators on rat prostatic cancer cell proliferation: comparison of strongly and weakly metastatic cell lines. *Prostate.* **44**, 61-76.

Frey, A. H. (1993). Electromagnetic field interactions with biological systems. *FASEB J.* **7**, 272-281.

Friedl, P., Noble, P. B. and Zanker, K. S. (1993). Lymphocyte locomotion in three-dimensional collagen gels. Comparision of three quantitative methods for analysing cell trajectories. *J. Immunol. Methods* **165**, 157-165.

Fukuda, M., Shimizu, K., Okamoto, N., Arimura, T., Ohta, T., Yamaguchi, S. and Faupel, M. L. (1996). Prospective evaluation of skin surface electropotentials in Japanese patients with suspicious breast lesions. *Jpn. J. Cancer Res*. **87**, 1092-1096.

Gardiner, R. A., Samaratunga, M. L., Gwynne, R. A., Seymour, G. J. and Lavin, M. F. (1996). Abnormal prostatic cells in ejaculates from men with prostatic cancer – a preliminary report. *Br. J. Urol*. **78**, 414-418.

Grimes, J. A. and Djamgoz, M. B. A. (1998). Electrophysiological characterization of voltage-activated Na^+ current expressed in the highly metastatic MAT-LyLu cell line of rat prostate cancer. *J. Cell Physiol*. **369**, 290-294.

Grimes, J. A., Fraser, S. P., Stephens, G. J., Downing, J. E., Laniado, M. E., Foster, C. S., Abel, P. D. and Djamgoz, M. B. A. (1995). Differential expression of voltage-activated Na^+ currents in two prostatic tumor cell lines: contribution to invasiveness in vitro. *FEBS Letts.* **369**, 290-294.

Gross, D. (1988). Electromobile surface charge alters membrane potential changes induced by applied electric field. *Biophysics* **54**, 879-884.

Gruler, H. and Nuccitelli, R. (1991). Neural crest galvanotaxis: new data and novel approach to the analysis of both galvanotaxis and chemotaxis. *Cell Motil. Cytoskeleton* **19**, 121-133.

Heberle, J., Riesle, J., Thiedemann, G., Oesterhelt, D. and Dencher, N. A. (1994). Proton migration along the membrane surface and retarded surface to bulk transfer. *Nature* **370**, 379-382.

Hotary, K. B. and Robinson, K. R. (1990). Endogenous electrical curents an the resultant voltage gradients in the chick embryo. *Dev. Biol.* **140**, 149-160.

Isaacs, J. T., Isaacs, W. B., Feitz, W. F. and Scheres, J. (1986). Establishment and characterization of seven Dunning rat prostatic cancer cell lines and their use in developing methods for predicting metastatic abilities of prostatic cancers. *Prostate* **9**, 261-281.

Isom, L. L., Ragsdale, D. S., Jongh, K. S., Westenbroek, R. E., Reber, B. F. X., Scheuer, T. and Catterall, W. A. (1995) Structure and function of the β2 subunit of brain sodium channels, a transmembrane glycoprotein with a CAM motif. *Cell* **83**, 433-442.

Jaffe, L. (1977). Electrophoresis along cell membrane. *Nature* **265**, 600-602.

Jaffe, L. F. and Nucitelli, R. (1977). Electrical controls of development. *Annu. Rev. Biophys. Bioeng.* **6**, 445-476.

Korohoda, W. and Kurowska, A. (1970). Quantitative estimations of the thresholds of electrotactic responses in *Amoeba proteus*. *Acta Protozool*. **7**, 375-382.

Korohoda, W. and Madeja, Z. (1997). Contact of sarcoma cells with aligned fibroblasts accelerates their displacement: computer assisted analysis of tumour cell locomotion in co-culture. *Biochem. Cell Biol.* **75**, 263-276.

Korohoda, W., Drukala, J., Sroka, J. and Madeja, Z. (1997a). Isolation, spreading, locomotion on various substrata, and the effect of hypotonicity on locomotion of fish keratinocytes. *Cell Motility Cytoskeleton* **38**, 38-53.

Korohoda, W., Golda, J., Sroka, J., Wojnarowicz, A., Jochym, P. and

Madeja, Z. (1997b). Chemotaxis of *Amoeba proteus* in the developing pH gradient within a pocket-like chamber studied with the computer assisted method. *Cell Motil. Cytoskeleton* **38**, 38-53.

Korohoda, W., Mycielska, M., Janda, E. and Madeja, Z. (2000). Immediate and long-term galvanotactic responses of *Amoeba proteus* to DC electric fields. *Cell. Motil. Cytoskeleton* **45**, 10-26

Laniado, M. E., Lalani, E. N., Fraser, S. P., Grimes, J. A., Bhangal, G., Djamgoz, M. B. A. and Abel, P. D. (1997). Expression and functional analysis of voltage-activated Na^+ channels in human prostate cancer cell lines and their contribution to invasion in vitro. *Am. J. Pathol.* **150**, 1213-1221.

Levine, M. D., Liotta, L. A. and Stracke, M. L. (1995). Stimulation and regulation of tumor cell motility in invasion and metastasis. *EXS* **74**, 157-179.

McCaig, C. D. (1989a). Nerve growth in the absence of cone filopodia and the effects of a small applied electric field. *J. Cell Sci.* **93**, 715-721.

McCaig, C. D. (1989b). Studies on the mechanism of embryonic frog nerve orientation in a small applied electric field. *J. Cell Sci*. **93**, 723-730.

McCaig, C. D. and Dover, P. J. (1993). Raised cyclic-AMP and small applied electric field influence differentiation, shape, and orientation of single myoblasts. *Dev. Biol.* **158**, 172-182.

McCaig, C. D. and Zhao, M. (1997). Physiological electric fields modify cell behaviour. *BioEssays* **19**, 818-826.

Meyer, R. L. (1982). Tetrodotoxin blocks the formation of ocular dominance columns in goldfish. *Science* **218**, 589-591.

Mohler, J. L. (1993). Cellular motility and prostatic carcinoma metastases. *Cancer Metastasis Rev.* **12**, 53-68.

Mohler, J. L., Partin, A. W. and Coffey, D. S. (1987). Prediction of metastatic potential by a new grading system of cell motility: validation in the Dunning R-3327 prostatic adenocarcinoma model. *J. Urol.* **138**, 168-170.

Mohler, J. L., Partin, A. W., Isaacs, J. T. and Coffey, D. S. (1988). Metastatic potential predication by a visual grading system of cell motility: prospective validation in the Dunning R-3327 prostatic adenocarcinoma model. **48**, 4312-4317.

Nishimura, K. Y., Isseroff, R. R. and Nuccitelli R. (1996). Human keratinocytes migrate to the negative pole in direct current electric field comparable to those measured in mammalian wounds. *J. Cell Sci*. **109**, 199-207.

Nuccitelli, R. (1988). Ionic currents in morphogenesis. *Experientia* **44**, 657-666.

Nuccitelli, R. **and Smart, T.** (1989). Extracellular calcium levels strongly influence neural crest cell galvanotaxis. *Biol. Bull.* **176** (Suppl), 130-135.

Olivotto, M. Arcangeli, A., Carla, M. and Wanke, E. (1996). Electric fields at the plasma membrane level: a neglected element in the mechanism of cell signaling. *BioEssays* **18**, 495-504.

Onuma, E. K. and Hui, S.-W. (1988). Electric field-directed cell shape changes displacement, and cytoskeletal reorganisation are calcium dependent. *J. Cell Biol*. **106**, 2067-2075.

Palmer, A. M., Messerli, M. A. and Robinson, K. R. (2000). Neuronal galvanotropism is independent of external Ca(2+) entry or internal Ca(2+) gradients. *J. Neurobiol*. **45**, 30-38.

Partin, A. W., Schoeniger, J. S., Mohler, J. L. and Coffey, D. S. (1989). Fourier analysis of cell motility with metastatic potential. *Proc. Natl. Acad. Sci. USA* **86**, 1254-1258.

Penn, A. A., Riquelme, P. A., Feller, M. B. and Shatz, C. J. (1998). Competition in retinogeniculate patterning driven by spontaneous activity. *Science* **279**, 2108-2112.

Perret, S., Cantereau, A., Audin, J., Dufy, B. and Georgescauld, D. (1999) Interplay between Ca^{2+} release and Ca^{2+} influx underlies localized hyperpolarization-induced [Ca^{2+}] waves in prostatic cells. *Cell Calcium* **25**, 297-311.

Price, J. A., Pethig, R., Lai, C. N., Becker F. F., Gascoyne, P. R. and Szent-Gyorgyi, A. (1987). Changes in cell surface charge and transmembrane potential accompanying neoplastic transformation of rat kidney cells. *Biochim. Biophys. Acta* **9**, 129-136.

Revest, P. A., Jones, H. C. and Abbott, N. J. (1993). The transendothelial DC potential of rat blood-brain barrier vessels in situ. *Adv. Exp. Med. Biol*. **331**, 71-74.

Robinson, K. R. (1985). The responses of cells to electrical fields: a review. *J. Cell Biol*. **101**, 2023-2027.

Rosado, J. A. and Sage, S. O. (2000) The actin cytoskeleton in store-mediated calcium entry. *J. Physiol*. **526**, 221-229.

Shatz, C. J. (1990). Impulse activity and the patterning of connections during CNS development. *Neuron* **5**, 745-756.

Scherrer, P. (1995). Proton movement on membranes. *Nature* **374**, 222.

Sheng, M. and Kim, E. (1996) Ion channel associated proteins. *Curr. Opin. Neurobiol*. **6**, 602-608.

Smith, P., Rhodes, P., Shortland, A. P., Fraser, S. P., Djamgoz, M. B. A., Ke, Y. and Foster, C. S. (1998). Sodium channel protein expression enhances the invasiveness of rat and human prostate cancer cells. *FEBS Lett*. **423**, 19-24.

Soong, H. K., Parkinson, W. C., Bafna S., Sulik G. L. and Huang, S. C. M. (1990). Movements of cultured corneal epithelial cells and stromal fibroblasts in electric fields. *Invest. Ophthalmol. Vis. Sci*. **31**, 2278-2282.

Stewart, D., Foster, C. S., Smith, P. and Djamgoz, M. B. A. (1999) Expression of voltage-gated Na^+ channels in human prostate cancer. *Soc. Neurosci. Abstr*. **25**, 208.

Szatkowski, M., Mycielska, M., Knowles, R., Kho, A.-L. and Djamgoz, M. B. A. (2000). Electrophysiological recordings from the rat prostate gland in vitro. Identified single cell and trans-epithelial (lumen) potentials. *BJU Int*. **86**, 1-8.

Wyckoff, J. B., Jones, J. G., Condeelis, J. C. and Segall, J. E. (2000) A critical step in metastasis: in vivo analysis of intravasation at the primary tumor. *Cancer Res*. **60**, 2504-2511.

Zhuang, H., Wang, W., Seldes, R. M., Tahernia, A. D., Fan, H. and Brighton, C. T. (1997) Electrical stimulation induces the level of TGF-beta1 mRNA in osteoblastic cells by a mechanism involving calcium/calmodulin pathway. *Biochem. Biophys. Res. Commun.* **6237**, 225-229.